Thin Solid Films 517 (2009) 1522–1529

Contents lists available at ScienceDirect

Thin Solid Films

journal homepage: www.elsevier.com/locate/tsf

Initial stages of deposition and film formation during spray pyrolysis — Nickel oxide, cerium gadolinium oxide and mixtures thereof

Ulrich P. Muecke *, Norman Luechinger, Lukas Schlagenhauf, Ludwig J. Gauckler [1]

ETH Zurich, Department of Materials, Nonmetallic Inorganic Materials, Wolfgang-Pauli-Str. 10, CH-8093 Zurich, Switzerland

ARTICLE INFO

Article history:
Received 13 October 2006
Received in revised form 22 June 2008
Accepted 12 August 2008
Available online 22 August 2008

Keywords:
Ceramics
Deposition process
Nickel oxide
Cerium gadolinium oxide
Spray pyrolysis

ABSTRACT

The formation of nickel oxide (NiO), cerium gadolinium oxide (CGO) and NiO–CGO thin films by air blast spray pyrolysis was studied at two scales. First, single droplets of precursor were deposited on sapphire substrates and the morphology of the formed residue was studied as a function of the substrate surface temperature, type of metal salt, salt saturation, and organic solvent in the precursor. Second, the synthesis of continuous films from repetitively deposited droplets and crack formation in the films were studied as a function of substrate temperature and salt decomposition kinetics. Nitrates, acetates, perchlorates and chlorides of nickel, cerium and gadolinium were the metal salts used, and mixtures of ethanol or water with di-, tri- and tetraethylene glycol were used as solvents.

Regular ring- or disc-shaped deposits were formed from single droplets that evaporated without boiling and were mainly observed with metal acetate- and chloride-based spray solutions or at low substrate temperatures. Disc-shaped residues were obtained for saturated salt solutions and changed to rings with diminishing rim thickness with decreasing salt saturation. The formation of bubbles in the droplet from boiling or salt decomposition during evaporation resulted in the distortion of the circular shape and was predominantly observed for metal nitrate-based precursors and at high substrate surface temperatures.

Continuous, dense and crack-free films of CGO and NiO–CGO with thicknesses up to 500 and 800 nm, respectively, were prepared from metal nitrate/chloride mixtures in a tetraethylene glycol-based solvent. The maximum crack-free thickness decreased with decreasing deposition temperature and was correlated to the metal salt decomposition kinetics.

1. Introduction

Spray pyrolysis can be used for the preparation of thin films for solar cells [1–3], electro-optic coatings [4–6], ferroelectric memory [7], insulating barrier layers [8,9], catalytically active coatings [10] or solid oxide fuel cell (SOFC) materials. Within the area of SOFC research, the method was mainly used to spray dense yttria or calcia stabilized zirconia [11–16], cerium gadolinium oxide (CGO) electrolyte thin films [17], interconnector films [18] or porous cathode structures [19]. Only recently, NiO–CGO composite films were prepared by spray pyrolysis as anode materials for SOFCs [20,21]. The fabrication of pure nickel oxide thin films by spray pyrolysis was extensively studied for the application in electrochromic or semiconducting devices [22–26].

The formation of a metal oxide thin film by spray pyrolysis involves the atomization of a liquid precursor containing metal salts, droplet transport towards a heated substrate and film formation on the substrate surface. Depending on the deposition temperature and precursor properties, the sprayed droplets and the metal salt decomposition products can either evaporate completely and a film is formed in a pseudo-chemical vapor deposition process [27] or (nano)particles are formed from the precursor droplets that are deposited on the substrate as solids [13]. Only when the substrate surface temperature is lower than the Leidenfrost point, liquid droplets are deposited on the surface [20]. The latter case will be studied here. After the liquid droplet impacts on the substrate, it wets the surface, spreads and is pinned along its perimeter to the surface. During or after the spreading process, solvents in the precursor start to evaporate and metal salt or decomposition intermediates might precipitate from the droplet when the saturation limit is reached [19]. The salts or precipitates decompose while the droplet is still liquid or after all solvents have evaporated, forming a single solid residue of metal oxide on the surface. The surface coverage of the substrate with deposits gradually increases with increasing deposition time and eventually a continuous film is formed [28].

The film quality, i.e. homogeneity or porosity, is not only influenced by the spray parameters like temperature or precursor flow rate, but also by the shape of the individual deposits. When a gas-tight layer is required, i.e. as a SOFC electrolyte, the film and consequently also the individual deposits have to be pore-free. Furthermore, the droplets

* Corresponding author. Tel.: +41 44 633 6841; fax: +41 44 632 1132.
E-mail addresses: ulrich.muecke@mat.ethz.ch (U.P. Muecke), ludwig.gauckler@mat.ethz.ch (L.J. Gauckler).
[1] Tel.: +41 44 632 5646; fax: +41 44 632 1132.

0040-6090/$ – see front matter © 2008 Published by Elsevier B.V.
doi:10.1016/j.tsf.2008.08.115

Table 1
Metal salts used for the preparation of the precursors

Salt	Purity	Solubility in water [g/ml (mol/l)]
Nickel-II-nitrate*$6H_2O$	98% [1]	3.5 (12.0) at 25 °C
Nickel-II-acetate*$4H_2O$	99% [1]	0.25 (1.0) at 25 °C
Nickel-II-perchlorate*$6H_2O$	98% [1]	2.9 (7.9) at 25 °C
Nickel-II-chloride*$6H_2O$	98% [1]	2.54 (10.7) at 20 °C [29]
Nickel-II-bromide*$3H_2O$	98% [1]	n. a.
Cerium-III-nitrate*$6H_2O$	99.5% [3]	1.754 (4.0) at 25 °C [29]
Cerium-III-acetate*$1.5H_2O$	99.9% [2]	0.1 (0.3) at 25 °C [30]
Ammonium-cerium-IV-nitrate	98% [1]	1.41 (2.6) at 25 °C [31]
Gadolinium-III-nitrate*$6H_2O$	99.9% [3]	n. a.
Gadolinium-III-chloride*$6H_2O$	99.9% [3]	n. a.
Gadolinium-III-acetate*$4H_2O$	99.9% [3]	0.14 (0.34) at 25 °C

Suppliers: [1]Fluka, Buchs, CH; [2]Aldrich, Steinheim, DE; [3]Alfa Aesar, Karlsruhe, DE.

have to impact evenly distributed to obtain full substrate coverage without leaving voids between the individual deposits.

Most publications on spray pyrolysis report only the morphology of the film after the deposition process is complete, neglecting the morphological features of the single deposits. The aim of this paper was, therefore, to study the morphology of single deposits and their spatial distribution on the substrate surface during spray pyrolysis. The deposit shape was correlated with the decomposition behaviour of the metal salts, the evaporation kinetics of the precursor droplet, the metal salt saturation and the solvent composition of the precursor. Additionally, the metal salt decomposition kinetics were investigated and correlated with crack formation during spraying. Based on the findings, a parameter set for the preparation of crack-free and dense CGO electrolyte and NiO–CGO anode thin films for SOFCs was exemplarily selected.

2. Experimental details

2.1. Spray pyrolysis setup

The same spray pyrolysis setup as described earlier [20] was used for all experiments. The distance between the spray nozzle tip and substrate surface was 39 cm and the air pressure was 0.1 MPa. The majority of the sprayed volume was transported by droplets with diameters between 5 and 50 μm. The substrate surface temperatures were in the range from 250 to 390 °C.

All films were deposited on 1 mm thick, 10 mm diameter sapphire single crystals (Stettler, Lyss, CH) with an (1120) orientation parallel to the surface. The substrates were cleaned with ethanol prior to deposition.

2.2. Precursor preparation and properties

Table 1 lists the metal salts used in this study. The precursor solutions were prepared by first dissolving one or more metal salts in ethanol (abbreviated E, 99.8%, Merck, Damstadt, DE or Scharlau, Barcelona, ES) or deionized water (W, 570 MΩ·cm, Nanopure deionizer, Barnstead Thermolyne, Dubuque, IA, USA) under constant stirring at 25–50 °C. The crystal water content of all salts was verified by thermogravimetry. After complete dissolution, a high boiling point solvent was added to the solution in volume ratios ranging from 1:9 to 2:1 ethanol or water to high boiling point solvent. Diethylene glycol (DEG, 99% purity, Acros, Geel, BE), triethylene glycol (TEG, 99%, Acros) and tetraethylene glycol (4EG, 99%, Aldrich, Steinheim, DE) were used as high boiling point solvents. The formation of a precipitate was observed for some metal acetates in combination with water and either TEG or 4EG. DEG constituted a good compromise as stable solutions were formed with all solvent/metal salt combinations used here. All precursors, where not otherwise noted, were precipitate free during the experiments and no appreciable change in colour or viscosity was observed. The total concentration of metal salts ranged from 0.01 mol/l to 1 mol/l and was limited by the solubility of the salts in ethanol or water. The solubility of the metal salts was always higher in ethanol or water than in the high boiling point solvent.

2.3. Characterization

The surface morphologies of the deposits were analyzed with a light microscope equipped with a digital camera (Polyvar MET, Reichert-Jung/DC300, Leica Microsystems, Wetzlar, DE) and by scanning electron microscopy (SEM, LEO 1530, Carl Zeiss SMT, Oberkochen, DE). Film thicknesses were measured by scratching off a small area of the film with a scalpel and measuring the step height between the substrate and an averaged height within about 1 mm scan length of the film with a surface profiler (Alpha Step 500, KLA Tencor, San Jose, CA, USA).

3. Results and discussion

Single separated droplets of precursors containing a nickel, cerium or gadolinium salt and mixtures thereof were sprayed on a heated substrate. The type of salt, the salt saturation, the ratio between low and high boiling point solvents and the substrate temperature were varied. The shape of single deposits was studied to investigate the evaporation and decomposition behaviour of the droplets after impact.

Deposits from nickel chloride- and nickel bromide-based solutions absorbed water from the surrounding air within 1 h after deposition at 390 °C and afterwards were easily wiped of the surface. This behaviour was linked to the incomplete thermal decomposition of the halide salts. Nickel bromide and chloride dehydrate between 200 and 300 °C to form hygroscopic intermediates that are stable up to 500 °C and 700 °C respectively [32]. The deposits that were composed of the intermediates rapidly regained crystal water after deposition, resulting in the wet deposits observed. Annealing of wet films yielded porous structures or cracked films. Porous NiO films from nickel chloride-based precursors were also reported by others [23,26]. Precursor solutions of pure nickel halides were, therefore, not studied in this work for the production of dense and crack-free NiO films.

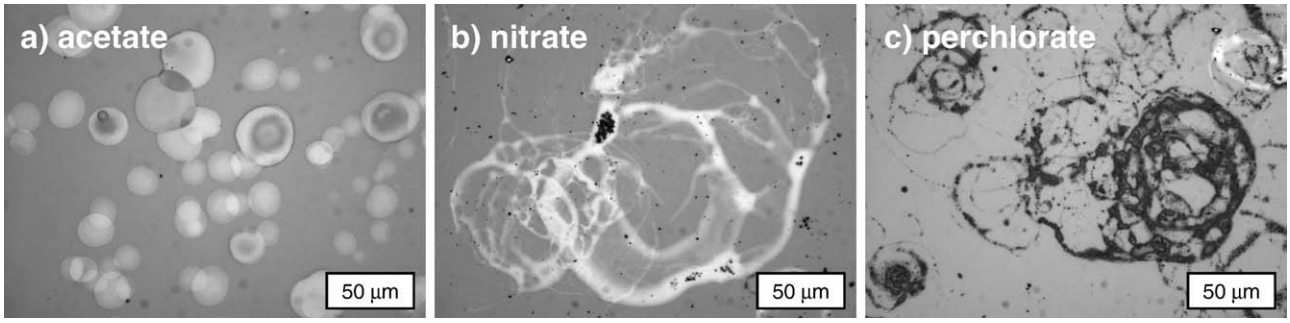

Fig. 1. Light microscope images of the morphology of single deposits from precursors with a) nickel acetate, b) nickel nitrate and c) nickel perchlorate (0.1 mol/l, 1:9 W:DEG, 330 °C, 30 ml/h, 1 min).

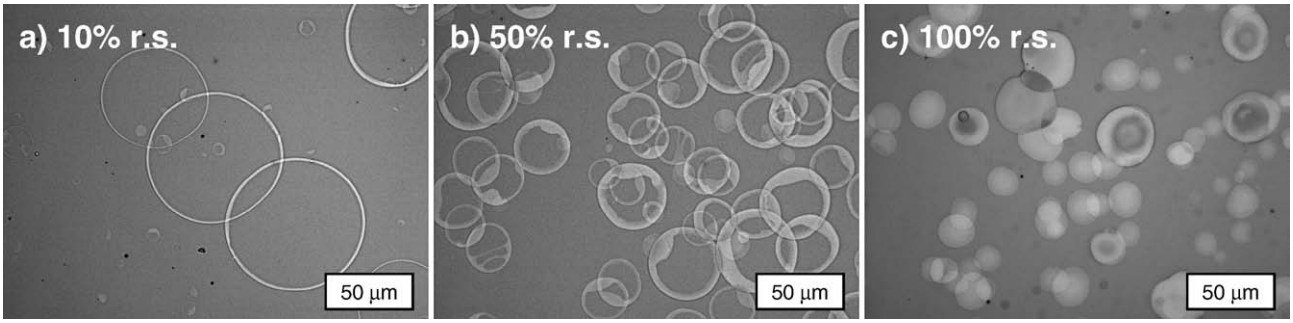

Fig. 2. Light microscope images of a nickel acetate-based precursor with different relative saturations (r. s.) (1:9 W:DEG, 330 °C, 30 ml/h, 1 min).

3.1. Deposition of nickel oxide

This section will mainly focus on the different types of single droplet deposits that can be achieved by varying the precursor properties or spray conditions. The formation of continuous films is discussed in the Sections 3.2 to 3.4.

3.1.1. Nickel salt

To study the influence of the type of metal salt on the shape of individual nickel oxide deposits, precursors containing different nickel salts were deposited under the same spray conditions. Nickel acetate, nickel nitrate and nickel perchlorate with a concentration of 0.1 mol/l were used in a solvent mixture of 1:9 W:DEG. The deposition time was 1 min, the flow rate 30 ml/h and the surface temperature 330 °C.

Depending on the salt, two types of deposits were observed: (1) regularly shaped discs or rings with a very wide rim (Fig. 1a) for the nickel acetate precursor and (2) irregularly shaped deposits from the nickel nitrate and perchlorate precursors (Fig. 1b and c).

The differences in residue morphology were linked to the evaporation and boiling behaviour of the precursor solutions. Droplets from the nitrate or perchlorate precursor were distorted by gas bubbles that evolved during evaporation and solidification of the droplet, leaving an irregularly shaped residue on the substrate surface. Bubble formation was observed at two length scales: large bubbles distorted the circular shape of the droplet on the hot substrate while evaporating (Fig. 1b) and small bubbles created numerous small spherical voids in thick areas of deposits (see the marked areas in Fig. 3). Very similar residue morphologies were reported by Cui et al. [33] for single evaporating droplets of an aqueous sodium carbonate solution in which gaseous carbon dioxide evolved during evaporation.

Regularly shaped discs or rings were formed when the droplets did not bubble shortly before solidification of the deposit, leaving an undistorted circular residue on the surface.

The disc type morphology is desirable for the preparation of dense films as the area under each deposit is completely covered by a metal salt residue and only few layers of deposits are required to obtain a full coverage of the substrate surface with a continuous film. Each deposit of the bubbling type morphology contains areas that are not covered by film and, consequently, more layers of droplets are needed until full coverage is obtained. In the following, the origin of the disc type morphology is further investigated and the formation of dense, crack-free and evenly thick films from the different droplet morphologies is studied.

3.1.2. Salt saturation

To examine the influence of the salt saturation on the deposit shape, nickel acetate and nitrate 1:9 W:DEG precursors with different relative salt saturations were deposited at the same spray conditions as above.

The morphology of the nickel acetate-based precursor changed from regular discs to rings with thick rims and then to rings with extremely thin rims (Fig. 2) when the relative saturation was decreased from 100% (0.1 mol/l) to 50% (0.05 mol/l and 10% (0.01 mol/l). The given relative saturations correspond to the saturations of nickel acetate in water at room temperature as the salt solubility in DEG is negligible. A very similar disc type morphology was also reported by Perednis [34] for a chemically similar precursor with the metal salt concentration close to the saturation limit.

A similar effect of relative saturation was observed for a nickel nitrate-based precursor. The residue morphology changed from a bubbling type to a disc and thick-rimmed ring type upon increasing the salt concentration from 0.1 mol/l (Fig. 3a) to 1.2 mol/l (Fig. 3b), corresponding to ~8.3% and ~100% saturation of nickel nitrate in water at room temperature.

Few of the thickest areas of the 0.1 M nickel nitrate precursor (marked area in Fig. 3a) and more than 50% of all discs and rings of the 1.2 M precursor (marked areas in Fig. 3b) contained trapped bubbles with diameters in the 1 µm range (Fig. 3c). The absence of irregularly shaped deposits of the 1.2 M precursor indicates that the salt concentration changed the evaporation and boiling behaviour of the droplet.

Although the metal salt saturation of the precursor might change slightly when the droplet is heating during the deposition process, it can be concluded that disc type deposits are formed if the metal salt

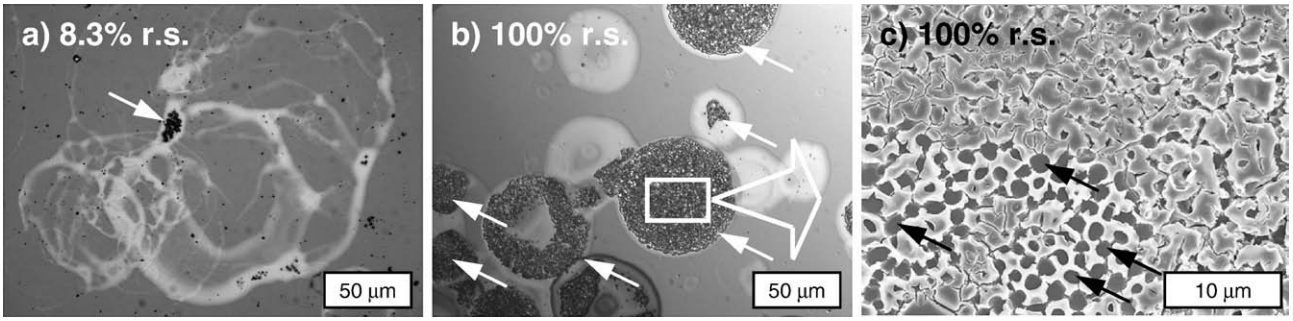

Fig. 3. Light microscope images of a nickel nitrate-based precursor with different relative salt saturations of a) 8.3% (0.1 mol/l), b) 100% (1.2 mol/l). Porous areas are marked with white arrows. c) Magnified SEM top view of porous areas with trapped bubbles (black arrows) of the 1.2 M precursor (all 1:9 W:DEG, 330 °C, 30 ml/h, 1 min).

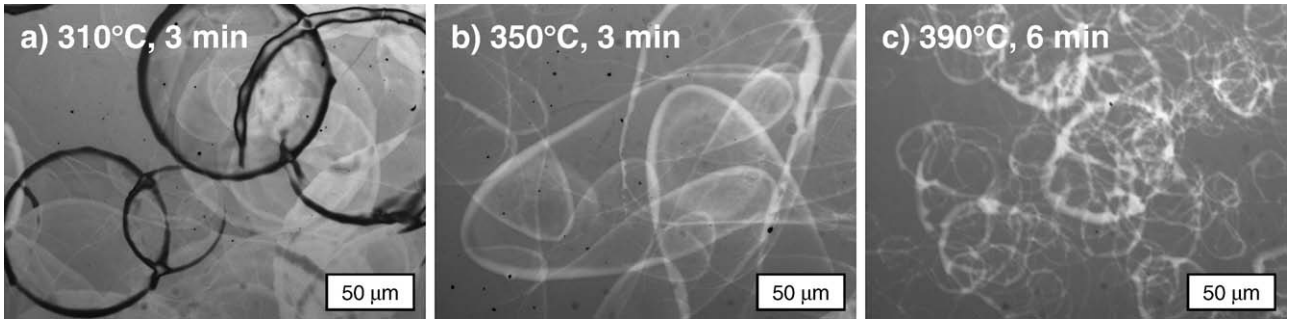

Fig. 4. Light microscope images of deposits from a 4EG-based nickel nitrate precursor sprayed at different substrate surface temperatures (0.1 mol/l, 1:9 W:4EG, 5 ml/h, spray times indicated).

concentration in the precursor is near the saturation limit before or during spraying. The morphology changes to a ring type or irregular shaped (=bubbling) type with lowered salt saturations. As a consequence, the desired deposit shape can be adjusted by choosing the salt saturation and type of salt. The disc thickness, for example, can be changed by varying the water to high boiling point solvent ratio while retaining full salt saturation in water.

3.1.3. Deposition temperature

The deposition temperature is one of the most important parameters in spray pyrolysis. A maximum substrate surface temperature, above which the deposition ceases completely, is generally observed [19,20]. The maximum deposition temperature for a 0.1 M 1:9 E:DEG-based precursor on sapphire is 350 °C and for a 0.1 M 1:9 E:4EG-based precursor 430 °C [20]. The maximum deposition temperature does not change if ethanol is exchanged with water.

Nickel acetate- and nickel nitrate-based precursors with DEG and 4EG were sprayed within a range of temperatures below the maximum deposition temperature to reveal how the evolution of the bubbling and disc type morphologies depend on the substrate temperature.

3.1.3.1. Nickel acetate. The deposit shape changed from a disc type at 330 °C to a ring type at 250 °C for a 0.1 M 1:9 W:DEG nickel acetate precursor. The liquid droplets spread to a different extent after impact and the average diameter of the residues increased from 30 µm at 330 °C to 60 µm at 250 °C. The width of the ring rims increased with increasing temperature up to the disc shape at 330 °C, indicating that the salt saturation in the droplet is a function of the substrate temperature and increases with increasing temperature due to solvent evaporation during droplet flight and spreading.

A similar behaviour was observed for a 0.1 M 1:9 W:4EG nickel acetate precursor. The deposits were of thick-rimmed ring type at 390 °C, indicating that the solubility of nickel acetate is larger in 4EG than in DEG. The average deposit diameter increased from 40 µm at 390 °C to 70 µm at 310 °C and the rim width increased towards higher temperatures. No evidence for bubbling was observed for any of the acetate precursors in the given temperature ranges.

3.1.3.2. Nickel nitrate. Deposits from a 0.1 M nickel nitrate 1:9 W:DEG precursor were of (distorted) ring type up to 250 °C and of bubbling type between 270 and 330 °C. The first trapped bubbles in thick parts of the deposits became visible at 320 °C and above.

The deposits of a 0.1 M 1:9 W:4EG nickel nitrate-based precursor were of ring type between 270 and 310 °C (Fig. 4). U-shaped and V-shaped residues were observed at temperature between 330 °C and 350 °C, indicating that the evaporating droplets were moving on the surface while evaporating. The droplet movement originated from solvent evaporation and not from aerodynamic forces because the droplet traces were randomly oriented. The deposits were of bubbling and V-shaped type in an equal ratio at 370 °C and of bubbling type at 390 °C. No trapped bubbles were observed at any of the temperatures.

3.1.4. Evaporation of macroscopic versus microscopic droplets

Up to here, the origin of the different deposit shapes was deduced from light microscope observations of the droplets after evaporation and decomposition because in-situ observation is difficult due to fast evaporation rates and small droplet sizes. However, as the evaporation behaviour of a droplet on a heated surface is largely independent of the droplet size [35], macroscopic precursor droplets can be used as model system to study the evaporation behaviour of micron-sized droplets, similarly to a previous study [20]. Millimetre-sized droplets were, therefore, deposited from a distance of 50 mm on a hot substrate by means of a pipette, and their evaporation behaviour was observed.

Droplets of 1:9 W:DEG or 1:9 W:4EG solvent mixtures without salts evaporated within less than 1 s under vigorous boiling when the substrate temperature was 330 and 390 °C, respectively. At lower temperatures when the evaporation time was larger than several seconds, heavy bubbling for ~1 s due to water evaporation followed by a period of calm evaporation due to high boiling point solvent evaporation was observed for these mixtures. The pure solvents evaporated calmly at temperatures below 330 and 390 °C, respectively. The irregular shaped morphology of the nickel nitrate precursors can, therefore, be caused by water evaporation. In case of the 1:9 W:4EG nickel nitrate precursor at 390 °C (Fig. 4), water evaporation was most likely the cause for the deposit distortion.

However, as no distortions were observed for the nickel acetate-based precursors at the same conditions and for the nickel nitrate-based precursor close to the salt saturation limit, the type of salt and salt saturation also influenced the boiling behaviour of the droplet and, consequently, the deposit shape.

From these results it can be concluded that not a single precursor property but a complex superposition of different effects determines the morphology of a single deposit. Ring or disc-shaped deposits are formed when the droplet solidifies while bubbles from solvent evaporation or salt decomposition are absent. When the salt decomposition is much slower or faster than the solvent evaporation, gaseous salt decomposition products can evolve from the droplet before or after the deposit has solidified, leaving the circular shape of the droplet undisturbed. It is also possible that the type of salt or the salt saturation suppresses boiling of the precursor.

Irregularly shaped deposits are formed when the low boiling point solvent evaporates under boiling while the residue is solidifying or when the salt decomposition time is on the order of the solvent evaporation time. Gaseous reaction products then evolve during solidification, causing a distortion of the circular droplet shape.

Bubbles within the residues are observed when the solidification of the residue occurs while gases from decomposing salt form small bubbles, trapping the gas in the deposit. Deposits with and without trapped bubbles were observed on the same sample because of the broad droplet size distribution in the spray and the associated different evaporation times. Trapped bubbles can be avoided by changing the difference between the solvent boiling point and salt decomposition temperature (see below) so that

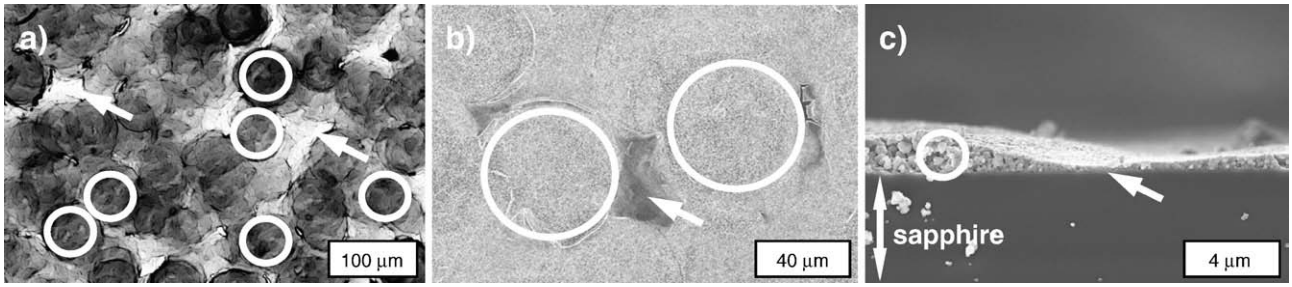

Fig. 5. a) Transmission light microscope image of as-deposited nickel acetate-based film with stacking of droplets (some thick areas circled, thin areas arrowed), b) SEM top view and c) SEM cross section. (0.1 mol/l, 1:9 W:DEG, 330 °C, 2 ml/h, 15 h, b) and c) annealed at 1000 °C for 10 h).

solvent evaporation and salt decomposition occur at different time scales.

3.2. Continuous films from single deposits

Films with average thicknesses between 200 and 1000 nm were deposited from precursors with different droplet morphologies and the film quality in terms of substrate coverage, thickness homogeneity and crack-freeness was investigated.

3.2.1. Stacking of droplets

Not only the shape of the deposits, but also an even distribution on the substrate, is important for films with homogeneous thicknesses. During spraying of continuous films from DEG-based precursors, the deposits did not distribute randomly on the substrate surface. In contrast, a selective deposition of droplets in circular areas was found. The films exhibited a nobby surface with the highest parts having a thickness of ~2 µm whereas no film or a thin layer of not more than 200 nm was found between the nobs (Fig. 5). The average diameter of the thick areas corresponded roughly to the average diameter of the deposits.

The thickness variations were observed for 0.1 M 1:9 E:DEG and 1:9 W:DEG precursors with nickel nitrate, acetate or perchlorate at 330 °C. The surface roughness decreased with decreasing temperature and the films were homogeneous below 290 °C for 0.1 M 1:9 W:DEG nitrate and acetate precursors.

The formation mechanism of the uneven film surface structure could be observed in a series of experiments with increasing spray times, starting with a blank substrate: after the first minutes of spraying, the substrate surface was randomly occupied with separate deposits and the surface coverage was less than one monolayer. However, successively arriving droplets selectively deposited on top of the first deposits rather than being deposited randomly, and stacks of deposits were formed on the surface.

The origin of the selective deposition was further investigated with regard to the Leidenfrost phenomenon: droplets of a pure liquid deposited on a hot substrate levitate on a vapor cushion above a certain temperature, called the Leidenfrost temperature. The droplets are mobile during the levitation period and might deposit on already existing obstacles on the surface.

Others have shown that the Leidenfrost temperature of micron-sized droplets is comparable to that of millimeter-sized droplets [20,35–37]. Macroscopic droplets can, therefore, be used to mimic the impact and spreading behaviour of the droplets in the spray.

For this purpose, several droplets of a 0.1 M 1:9 W:DEG nickel nitrate precursor were deposited on a substrate at 330 °C by means of a pipette. On a clean substrate, the droplets levitated for 1–2 s, moved around on the surface and then deposited at a random position under heavy boiling and distortion of the droplet, leaving residues from salt decomposition on the surface. Successively deposited droplets also levitated but deposited selectively at the positions of previously formed residues. Decreasing the substrate temperature shortened the levitation period until all droplets were deposited directly. This would also explain why stacking is most pronounced at substrate temperatures close to the Leidenfrost temperature (~350 °C for 0.1 M 1:9 W:DEG-based precursors) where most of the droplets levitate and why no stacking is observed at temperatures below 290 °C for DEG-based precursors.

Other authors [17,19,34] reported that films without stacking can be prepared from precursors with ethanol or water volume fractions of >30%. Nickel nitrate-based precursors with a concentration of 0.1 mol/l and a solvent ratio of 1:2 E:DEG and 2:1 E:DEG were deposited at different temperatures to investigate the influence of the solvent ratio on the residue morphology and stacking behaviour. The morphology changed from an irregular bubbling type to a ring type with increasing amount of low boiling point solvent. The residue morphology was unaffected when water was replaced by ethanol and the stacking phenomenon was observed for both solvents. The tendency towards stacking decreased with increasing ethanol or water content and with decreasing substrate temperature.

3.2.2. Crack-free NiO films

All NiO films from 1:9 W:DEG nickel acetate precursors were cracked at temperatures below 320 °C and before full substrate coverage at 100–200 nm thickness was obtained. Films from 1:9 W:DEG nickel nitrate precursors that contained trapped bubbles in the deposits were crystalline after annealing at 1000 °C for 10 h with an average grain size of 265 nm [21]. However, the pore structure from the single deposits was retained even after annealing. Due to cracking, porosity and the stacking phenomenon, DEG-based precursors were not further investigated for the preparation of films.

Films prepared with a 1:9 W:4EG nickel acetate precursor were crack-free up to a thickness of 400 nm, the substrate was fully covered and no stacking was observed. No trapped bubbles were visible in the deposits and, consequently, in the film. The temperature was 390 °C, the flow rate 5 ml/h and the spray time 90 min.

Nickel nitrate-based films with a 1:9 E:4EG or W:4EG solvent were crack-free up to a thickness of 800 nm at 390 °C with a flow rate of 5 ml/h and 120 min spray time. No trapped bubbles and no cracks were observed and the film was homogeneous in thickness.

The 4EG-based precursors were, therefore, most suitable for the preparation of crack-free and dense films from nitrate and acetate salts.

3.2.3. Crack formation and salt decomposition

Besides inhomogeneous film thicknesses, cracks were frequently observed during film deposition or after a subsequent temperature treatment of the films, i.e. NiO films from 1:9 W:DEG nickel acetate precursors. However, films with a nickel nitrate precursor were crack-free (although stacked) up to a thickness of ~2 µm at the same deposition conditions. The influence of the type of salt on the crack formation was, therefore, further investigated.

The mechanism of crack formation can be understood as a step-by-step process. An impacting droplet spreads on the substrate surface, is

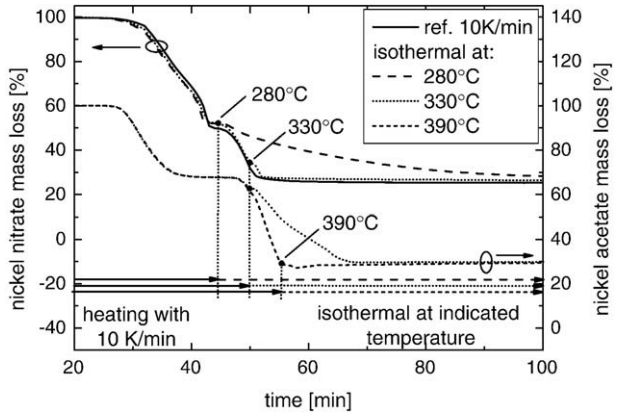

Fig. 6. Thermogravimetric analysis of the decomposition kinetics of nickel nitrate and nickel acetate heated to 280 °C, 330 °C and 1000 °C and 330 °C, 390 °C and 1000 °C respectively with 10 K/min and held at the respective temperature for 1 h. The temperature ramp was started at t=20 min and 30 °C.

heated and the solvent starts to evaporate. When the saturation limit is reached, metal salt or salt decomposition intermediates may precipitate in the droplet and the remaining solvent evaporates, leaving a residue on the surface. The decomposition of the salt or salt intermediate can start at any point during the deposition if the temperature is sufficiently high. Once the deposit is attached to the substrate and is unable to shrink in diameter, the shrinkage associated with salt decomposition causes tensile stresses in the deposits. The stresses build-up with every deposited droplet and the film will ultimately crack when the fracture strength of the material is exceeded. Spray pyrolysis films are, therefore, always tensile in stress.

Very smooth and crack-free films with a thickness of several micrometers can generally be prepared with any precursor if the substrate temperature is much below the maximum deposition temperature. However, these films all crack upon annealing and are often referred to as being “too wet” in the literature, meaning that some organic residues are left in the films that cause cracks during annealing. But these deposition temperatures are also low enough that most of the salt intermediates do not decompose during the deposition and the shrinkage and cracking is caused mainly by the stresses induced from salt decomposition during the subsequent annealing.

A general trend observed during spraying of all precursors in this study and also a previous work [20] was that the maximum obtainable crack-free film thickness of the same metal oxide was a function of the solvent boiling point. Precursors with chemically similar high boiling point solvents and otherwise identical parameters were sprayed at temperatures that resulted in similar evaporation times of the precursors. The thickest crack-free films were obtained with the highest boiling point solvent, 4EG, whereas films prepared with DEG cracked at 2/3 to 1/2 of that thickness. This suggests that the metal salt decomposition kinetics are important for the preparation of crack-free films with maximized thicknesses.

Fig. 6 illustrates the decomposition behaviour of nickel nitrate and nickel acetate isothermally held at 280 °C, 330 °C and 1000 °C; and 330 °C, 390 °C and 1000 °C, respectively. All samples were heated with 10 °C/min to the dwell temperature. The decomposition of the stable nickel nitrate intermediate formed around 280 °C proceeded over several hours and even at 330 °C, close to the final decomposition temperature around 400 °C, a kinetic behaviour is observable. The nickel acetate intermediate formed around 300 °C is stable for more than 20 min when held at 330 °C. The decomposition time is expected to be even longer under real spray conditions when the droplets are heated to the substrate temperature within milliseconds.

Assuming that the salt decomposition kinetics measured by thermogravimetry of the pure salt in air are comparable to that of the salt residue on the substrate, the salt decomposition is a very slow process compared to the solvent evaporation, which takes only several milliseconds. If the deposition temperature is much higher than the salt decomposition temperature, the salts will partly decompose in the still-liquid droplet without stress build-up. The tensile stresses during the final decomposition are reduced and larger maximum crack-free film thickness is possible. This might explain why the maximum crack-free film thickness is so different with chemically similar high boiling point solvents. A comparable mechanism was reported by some authors [38,39] for the preparation of sol–gel thin films. A flexible organic backbone of the deposited gel allows to keep the thin film viscous during salt decomposition, effectively reducing the stresses during shrinkage and increasing the maximum crack-free thickness.

3.3. Gadolinia doped ceria films

3.3.1. Cerium and gadolinium salts

Single cerium and gadolinium salts were sprayed to obtain the characteristic morphologies of these salts. The solution concentration was 0.01 mol/l for cerium and gadolinium acetate, 0.1 mol/l for cerium nitrate, cerium ammonium nitrate, gadolinium nitrate and gadolinium chloride in a solvent mixture of 1:9 W:DEG. The concentration of gadolinium acetate in water was at ~30% relative saturation and that of cerium acetate at ~33% relative saturation.

Cerium and gadolinium acetate-based precursors formed thick-rimmed ring type deposits, cerium nitrate and ammonium nitrate deposits were of bubbling type and the gadolinium chloride and nitrate were of ring type morphology. The same salt saturation dependency as for nickel acetate was found for cerium and gadolinium acetate with a transition from discs to thin-rimmed rings with decreasing metal salt concentration in water. Stacking was less pronounced for the cerium acetate-based solution compared to the nickel acetate precursor. The continuous films from cerium nitrate and cerium ammonium nitrate were very homogenous and some bubbles

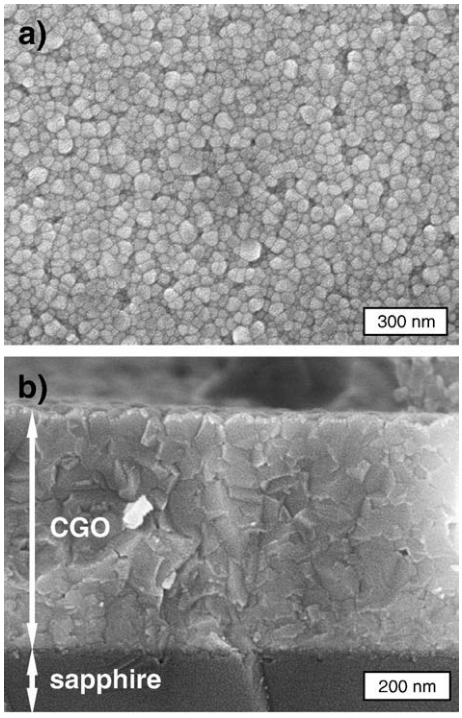

Fig. 7. a) SEM top view and b) cross section micrographs of a 560 nm thick CGO film on sapphire (0.1 mol/l, 1:9 W:4EG, cerium nitrate and gadolinium chloride, 390 °C, 5 ml/h, 60 min, film annealed at 1000 °C for 10 h).

were found in the rims of the deposits. Very pronounced stacking was present in all gadolinium salt derived films with some trapped bubbles in the rings for gadolinium nitrate and gadolinium chloride.

3.3.2. CGO films

To correlate continuous film formation with the single deposit shapes, $Ce_{0.8}Gd_{0.2}O_{1.9-x}$ electrolyte thin films were sprayed with precursors containing cerium and gadolinium acetate or cerium nitrate and gadolinium chloride.

Deposits sprayed with an acetate-based solution of 0.01 and 0.05 mol/l in 1:9 W:DEG were of thick-rimmed ring and disc type morphology, respectively, at 330 °C. Stacking was observed and the films were cracked before complete substrate coverage was obtained. Acetate-based precursors with 1:9 E:TEG, 1:9 W:TEG, 1:9 E:4EG and 1:9 W:4EG and a concentration of 0.05 mol/l were of thick-rimmed ring to disc type at 350 and 390 °C, respectively, with decreasing rim thickness when the concentration was decreased. These precursors were not suitable for film preparation from disc-shaped residues because a precipitate formed in the precursor 15–30 min after preparation. Spraying of the suspension resulted in porous and cracked areas within the deposits.

The deposits of a cerium nitrate and gadolinium chloride precursor with a concentration of 0.1 mol/l in 1:9 E:TEG were of bubbling type at 350 °C on sapphire. No stacking was observed but bubbles were trapped in the rims of the residues, resulting in porosity of the film after deposition. The maximum crack-free film thickness was 500 nm with some porosity in the film from trapped bubbles in individual deposits.

Deposits from a 0.1 M 1:9 W:4EG precursor (1:9 E:4EG was not stable) were of bubbling type with some V-shaped traces at 390 °C. No bubbles were found in the rims of the deposits, no stacking was observed and the films were dense after deposition. Crack-free layers and dense films up to 800 nm were prepared with the 4EG-based solution (Fig. 7). The flow rate was 5 ml/h, the deposition time 60–90 min and the temperature 390 °C. Using gadolinium nitrate instead of gadolinium chloride did not affect the residue morphology, density of the film or maximum possible crack-free film thickness.

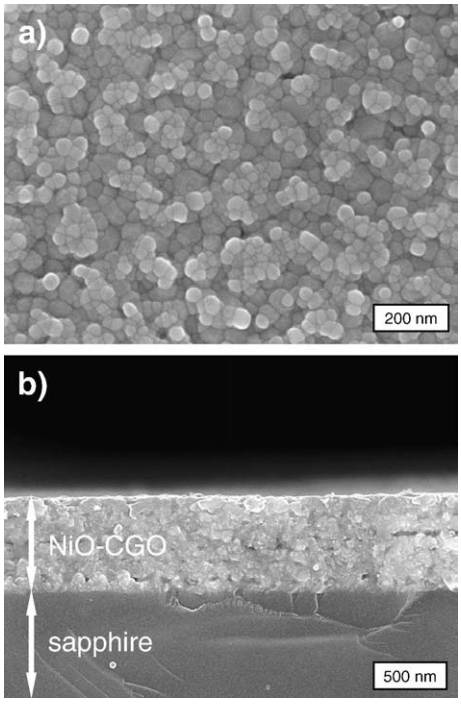

Fig. 8. a) SEM top view and b) cross section images of a 800 nm thick NiO–CGO film (0.1 mol/l, 1:9 E:4EG, nickel nitrate, cerium nitrate and gadolinium chloride, 390 °C, 5 ml/h, 150 min, film annealed at 1000 °C for 10 h).

These results show that the residue morphology of a salt mixture corresponds to that of the single salts if salts of the same morphological types are used. Porosity in the films can be avoided by proper choice of the single deposit morphology.

3.4. NiO–CGO films

NiO–CGO thin films were prepared to demonstrate the feasibility of dense and crack-free two-phase composite anode thin films by spray pyrolysis. The films were sprayed with a 0.1 M precursor containing nickel nitrate, cerium nitrate and gadolinium chloride with a solvent composition of 1:9 E:4EG. The targeted composition after reduction in hydrogen was 60 vol.% metallic nickel and 40 vol.% CGO.

The deposits were of bubbling and V-shaped trace morphology at a temperature of 390 °C. No bubbles within the rims of the deposits and no stacking was observed. Dense and crack-free films with a maximum thickness of 800 nm were obtained at 390 °C, a flow rate of 5 ml/h and 150 min deposition time (Fig. 8). No difference in deposit or film morphology was observed when gadolinium chloride was exchanged with gadolinium nitrate or when the Ni/CGO ratio was varied between 0/100 and 100/0.

NiO–CGO films from a 0.1 M 1:9 W:4EG- and 1:9 W:TEG-based precursor with nickel acetate, cerium acetate and gadolinium acetate were of thick-rimmed ring to disc type at 390 °C and 350 °C respectively. No bubbling was observed but stacking was very pronounced and cracking occurred before complete substrate coverage was obtained. Decreasing the salt concentration to 0.05 and 0.01 mol/l resulted in decreased ring rim thickness. Combining single salts of the same residue morphology again resulted in the same morphology for the salt mixture.

4. Summary and conclusion

Precursors with different nickel salts were used to study the morphology of single droplet deposits formed on a sapphire surface during spray pyrolysis. Three major morphological types of residues were distinguished: regular rings or discs, irregular shapes and V- or U-shaped traces. Regular rings or discs were formed when droplets evaporated without boiling on the surface during solidification or when gaseous reaction products from metal salt decomposition escaped before or after the droplet solidified. Regular rings turned into discs when the salt concentration was increased to the saturation limit of the salt in the precursor. Irregularly shaped residues were observed when the droplet was distorted during solidification because of solvent boiling or gaseous reaction products from salt decomposition evolving. V- or U-shaped traces were observed when evaporating solvent or evolving gases caused the droplets to move on the surface. Porosity can be introduced in the deposits when small bubbles are trapped in the rims of the deposit during solidification.

A non-random stacking of deposits was observed for some precursors. The phenomenon was tentatively associated with the Leidenfrost effect. Droplets can levitate for a period of several seconds above a hot surface before being deposited. The droplets are mobile during that period and preferentially deposit at sites where residues were formed previously.

Cracking of spray pyrolysis thin films was correlated to the salt decomposition kinetics. The shrinkage of a deposit that is pinned to the surface results in tensile stresses in the growing film that lead to fractures and is caused by the decomposition of metal salts. The stresses can be reduced when the salt decomposition occurs in large parts in the still-liquid droplet or when the deposit remains viscous after solvent evaporation and salt decomposition. The thickest crack-free films were, therefore, obtained from metal salts with a low decomposition temperature in combination with a very high boiling point solvent. Crack-free CGO and NiO–CGO films with a

thickness of up to 560 and 800 nm, respectively, were prepared with this approach.

Acknowledgements

Financial support from BFE under project number 100430, from KTI under project number 7085.2 DCPP-NW, from the European Union within the REAL-SOFC project and from ETH Zurich is gratefully acknowledged.

References

[1] B.J. Lokhande, P.S. Patil, M.D. Uplane, Physica. B 302 (2001) 59.
[2] B.J. Lokhande, P.S. Patil, M.D. Uplane, Mater. Lett. 57 (2002) 573.
[3] M.S. Tomar, F.J. Garcia, Prog. Cryst. Growth Charact. Mater. 4 (1981) 221.
[4] P.S. Patil, L.D. Kadam, Appl. Surf. Sci. 199 (2002) 211.
[5] L.D. Kadam, S.H. Pawar, P.S. Patil, Mater. Chem. Phys. 68 (2001) 280.
[6] D.S. Albin, S.H. Risbud, Adv. Ceram. Mater. 2/3A (1987) 243.
[7] G. Brankovic, Z. Brankovic, J.A. Varela, E. Longo, J. Eur. Ceram. Soc. 24 (2004) 989.
[8] X. Yi, W. Wenzhong, Q. Yitai, Y. Li, C. Zhiwen, Surf. Coat. Technol. 82 (1996) 291.
[9] I. Stambolova, K. Konstantinov, D. Kovacheva, M. Khristov, P. Peshev, T. Donchev, Mater. Lett. 30 (1997) 333.
[10] R.N. Singh, J.-F. Koenig, G. Poillerat, P. Chartier, J. Electroanal. Chem. 314 (1991) 241.
[11] T. Setoguchi, M. Sawano, K. Eguchi, H. Arai, Solid State Ionics 40–41 (1990) 502.
[12] P. Bohac, L. Gauckler, Solid State Ionics 119 (1999) 317.
[13] D. Perednis, L.J. Gauckler, J. Electroceram. 14 (2005) 103.
[14] D. Perednis, O. Wilhelm, S.E. Pratsinis, L.J. Gauckler, Thin Solid Films 474 (2005) 84.
[15] Y. Matsuzaki, M. Hishinuma, I. Yasuda, Thin Solid Films 340 (1999) 72.
[16] O. Wilhelm, S.E. Pratsinis, D. Perednis, L.J. Gauckler, Thin Solid Films 479 (2005) 121.
[17] J.L.M. Rupp, A. Infortuna, L.J. Gauckler, Acta Mater. 54 (2006) 1721.
[18] A. Furusaki, H. Konno, R. Furuichi, J. Mater. Sci. 30 (1995) 2829.
[19] D. Beckel, A. Dubach, A.R. Studart, L.J. Gauckler, J. Electroceram. 16 (2006) 221.
[20] U.P. Muecke, N. Lüchinger, L. Schlagenhauf, L.J. Gauckler, Thin Solid Films 517 (2009) 1515, doi:10.1016/j.tsf.2008.08.158.
[21] U.P. Muecke, S. Graf, U. Rhyner, L.J. Gauckler, Acta Mater. 56 (2008) 677.
[22] Xie Yi, Wang Wenzhong, Qian Yitai, Yang Li, Chen Zhiwen, J. Cryst. Growth 167 (1996) 656.
[23] L.D. Kadam, P.S. Patil, Sol. Energy Mater. 69 (2001) 361.
[24] S.A. Mahmoud, A.A. Akl, H. Kamal, K. Abdel-Hady, Physica. B 311 (2002) 366.
[25] H. Kamal, E.K. Elmaghraby, S.A. Ali, K. Abdel-Hady, Thin Solid Films 483 (2005) 330.
[26] B.A. Reguig, M. Regragui, M. Morsli, A. Khelil, M. Addou, J.C. Bernede, Sol. Energy Mater. 90 (2006) 1381.
[27] J.C. Viguie, J. Spitz, J. Electrochem. Soc. 122 (1975) 585.
[28] R. Neagu, D. Perednis, A.S. Principalle, E. Djurado, Chem. Mater. 17 (2005) 902.
[29] Merck, Merck ChemDAT, 2006.
[30] Molycorp Inc., A Lanthanide Lanthology, Molycorp Inc., Mountain Pass, CA, USA, 1993.
[31] T.-L. Ho, Encyclopedia of Reagents for Organic Synthesis, Wiley, New York, 1995.
[32] S.K. Mishra, S.B. Kanungo, J. Therm. Anal. Calorim. 38 (1992) 2417.
[33] Q. Cui, S. Chandra, S. McCahan, J. Heat Transfer 123 (2001) 719.
[34] D. Perednis, PhD thesis, Department of Materials, Swiss Federal Institute of Technology, Zurich, 2003.
[35] T.Y. Xiong, M.C. Yuen, Int. J. Heat Mass Transfer 34 (1991) 1881.
[36] J.D. Bernardin, I. Mudawar, C.B. Walsh, E.I. Franses, Int. J. Heat Mass Transfer 40 (1997) 1017.
[37] J.D. Bernardin, C.J. Stebbins, I. Mudawar, Int. J. Heat Mass Transfer 40 (1996) 73.
[38] H. Kozuka, J. Ceram. Soc. Jpn. 111 (2003) 624.
[39] C.J. Brinker, A.J. Hurd, P.R. Schunk, G.C. Frye, C.S. Ashley, J. Non-Cryst. Solids 147 (1992) 424.